Article

Current Biology

Spaced training enhances memory and prefrontal ensemble stability in mice

Highlights

- Spacing trials enhances memory, yet impairs learning in the "everyday memory" task
- The dorsomedial prefrontal cortex is activated during and is necessary for this task
- Ensemble activity patterns are more similar between subsequent spaced trials
- Trial spacing does not affect ensemble size

Authors

Annet Glas, Mark Hübener, Tobias Bonhoeffer, Pieter M. Goltstein

Correspondence

goltstein@neuro.mpg.de

In brief

Glas et al. show that increasing the time interval between trials affects learning and memory in mice. The memory-enhancing effect of trial spacing is accompanied by increased stability of the ensemble response pattern in the dorsomedial prefrontal cortex, whereas the ensemble size is unaffected.

Glas et al., 2021, Current Biology *31*, 4052–4061
September 27, 2021
https://doi.org/10.1016/j.cub.2021.06.085

CellPress

CellPress
OPEN ACCESS

Current Biology

Article

Spaced training enhances memory and prefrontal ensemble stability in mice

Annet Glas,[1,2] Mark Hübener,[1] Tobias Bonhoeffer,[1] and Pieter M. Goltstein[1,3,*]
[1]Max Planck Institute of Neurobiology, Am Klopferspitz 18, 82152 Martinsried, Germany
[2]Graduate School of Systemic Neurosciences, Ludwig-Maximilians-Universität München, Großhaderner Straße 2, 82152 Martinsried, Germany
[3]Lead contact
*Correspondence: goltstein@neuro.mpg.de
https://doi.org/10.1016/j.cub.2021.06.085

SUMMARY

It is commonly acknowledged that memory is substantially improved when learning is distributed over time, an effect called the "spacing effect". So far it has not been studied how spaced learning affects the neuronal ensembles presumably underlying memory. In the present study, we investigate whether trial spacing increases the stability or size of neuronal ensembles. Mice were trained in the "everyday memory" task, an appetitive, naturalistic, delayed matching-to-place task. Spacing trials by 60 min produced more robust memories than training with shorter or longer intervals. c-Fos labeling and chemogenetic inactivation established the involvement of the dorsomedial prefrontal cortex (dmPFC) in successful memory storage. *In vivo* calcium imaging of excitatory dmPFC neurons revealed that longer trial spacing increased the similarity of the population activity pattern on subsequent encoding trials and upon retrieval. Conversely, trial spacing did not affect the size of the total neuronal ensemble or the size of subpopulations dedicated to specific task-related behaviors and events. Thus, spaced learning promotes reactivation of prefrontal neuronal ensembles processing episodic-like memories.

INTRODUCTION

Extending the period between individual learning events can considerably strengthen a memory and increase its lifespan, a phenomenon called the "spacing effect".[1] This phenomenon has been described across a wide range of species, from mollusk to man.[2] In mice, spaced training can strengthen associative,[3] episodic-like,[4] motor,[5] and spatial[6] memories. The effectiveness of spacing learning is thought to be mediated by molecular and synaptic processes,[2] which involve activation and expression of key signaling proteins and transcription factors,[2,6,7] leading to increased synaptic plasticity.[5,8] It has not yet been studied whether and how increasing the spacing of learning events affects neuronal ensembles representing individual memories.

During a learning experience, a subset of neurons is activated as a result of their intrinsic excitability and external sensory drive.[9–12] The memory itself is thought to be encoded by synaptic connections that are newly formed or strengthened within this neuronal ensemble.[13–15] Subsequently, memories can be consolidated by further functional and structural synaptic remodeling, enabling long-term retention.[16,17] For retrieval of a memory, neurons that are part of the ensemble need to be reactivated in a pattern similar to that during memory encoding.[11,18,19]

The working hypothesis for the present work is that the molecular and synaptic mechanisms underlying the spacing effect[2] can influence two characteristics of neuronal ensembles, i.e., the size or reactivation pattern of the ensemble, during memory encoding, storage, and retrieval. The reasoning is that when learning occurs over multiple optimally spaced trials, molecular signaling initiated in the first trial can extend the temporal window of enhanced neuronal excitability[10,20] and thereby increase the likelihood of the same ensemble being reactivated in subsequent trials. As such, spaced training would more effectively strengthen the ensemble's internal synaptic connectivity[21,22] and by local competitive circuit interactions result in a sparser but more reliably activated assembly.[23–25] Sparseness would safeguard the specificity of the represented memory,[26] whereas stronger connectivity would render the memory more resilient to homeostatic mechanisms that can result in forgetting[27] and thereby increase the probability of retrieval. Conversely, as the group of excitable neurons drifts over time,[10] consecutive learning experiences could activate different sets of neurons. Spacing learning experiences over extended periods could therefore allocate a memory to overlapping sets of neurons.[28] Within this framework, the memory-enhancing effect of spaced training could be mediated by representing a learning experience with a larger neuronal ensemble.[4,11]

To determine whether and how trial spacing changes the way neuronal ensembles represent learned experiences, we implemented the "everyday memory" task, a naturalistic delayed matching-to-place task.[7] The instilled episodic-like memories are typically forgotten within 24 h, but spaced training reliably prolongs the period over which the memories can be recalled.[7] Efficient execution of the everyday memory task relies on functions that have been attributed to the dorsal medial prefrontal cortex (dmPFC), including behavioral flexibility[29] and learning against a background of relevant prior knowledge.[30] Moreover,

rodent PFC is, in concert with the hippocampus, involved in the encoding and retrieval of episodic-like memories,[31,32] providing an attractive system for examining the relation between neuronal ensemble activity and memory strength.

Here we report that trial spacing improves memory and is accompanied by enhanced reactivation of the neuronal ensembles in the dmPFC. Increasing trial spacing in the everyday memory task enhanced memory retrieval yet impaired memory encoding. *In vivo* calcium imaging with a miniaturized microscope revealed that trial spacing results in more similar reactivation of the ensemble between encoding trials (ETs) and upon memory retrieval. Conversely, trial spacing did not affect the number of activated neurons, suggesting that trial spacing primarily affects the synaptic strength within the neuronal ensemble but not its size.

RESULTS

Studying episodic-like memory in the everyday memory task

We trained female mice (n = 20) in repeated sessions of the everyday memory task (see STAR Methods; Figures 1A and 1B; Video S1).[7] Each training session consisted of three ETs) (separated by an "encoding intertrial interval") and three retrieval trials (RTs). During each ET, mice entered the radial arm maze from a start box, explored the maze, and retrieved a buried chocolate reward by digging in one of two available, odor-masked sandwells (i.e., the "rewarded" sandwell). Upon completion of the final ET, mice were kept in their home cage for an extended delay period ("retrieval delay"), after which the three RTs were conducted. During RTs, mice had to revisit the previously rewarded sandwell. Simultaneously, mice had to refrain from digging at the previously non-rewarded sandwell, as well as four new non-rewarded sandwells ("non-cued" sandwells). After each session, we changed the spatial configuration of the sandwells and the position of the start box. Consequently, mice had to relearn and remember a different rewarded location in each subsequent session. Performance in each trial was quantified as the number of incorrect sandwells the mouse dug in, relative to the total number of available sandwells (see STAR Methods).

We first characterized the conditions under which mice were able to successfully complete the task. Memory was only reliably retrieved after training with multiple ETs in which the rewarded location was kept constant (Figure S1). In sessions, performance increased across subsequent ETs, as well as subsequent RTs, verifying that mice can encode and retrieve memories in this task (Figure 1C). In addition, we studied the within- and between-session strategies that mice employ in this task. Altering the start box location between and after ETs confirmed that mice primarily used an allocentric (world-centered) rather than egocentric (body-centered) reference frame (Figures S2A–S2D).[33] Within a session, mice revisited non-rewarded arms less than expected from chance (Figure S2E) and focused their search progressively closer to the rewarded arm (Figure S2F). Between sessions, the previous session's retrieval performance did not affect the next session's retrieval performance (Figure S2G), suggesting that a successfully stored memory did not interfere with learning of a new memory. From these analyses, we conclude that mice employ both a "within-session win-stay" and a "between-session switch" strategy to optimize their task performance.

Increasing trial spacing enhances memory retrieval but impairs memory encoding

To examine the influence of trial spacing on encoding and retrieval of episodic-like memory, we tested the effect of four encoding intertrial intervals: 30 s (i.e., "massed" training, 119 sessions), 10 min (115 sessions), 30 min (133 sessions), and 60 min (132 sessions) (Figure 1B; Video S1). To probe the effect of trial spacing on same- and next-day memory retrieval separately, we conducted RTs after a retrieval delay of either 2.5 or 24 h. Performance was stable over months of training, allowing us to average a mouse's performance across sessions of the same encoding intertrial interval and retrieval delay.

We observed that performance in the second and third ET was reduced when encoding intertrial intervals were extended (Figure 1D). In addition, memory retrieval after 24 h was improved when encoding intertrial intervals were longer, yet no effect was observed after 2.5 h (Figure 1E). This difference was not unexpected because trial spacing primarily affects less recent memories.[2] As a control, we compensated for impaired encoding by normalizing the performance in the first RT to the encoding performance in the final, third ET ("retention"). Retention thereby addressed how much of the successfully encoded information persisted and subsequently could be retrieved. Memory retention positively correlated with encoding intertrial interval after both a 2.5- and 24-h retrieval delay.

In a subset of sessions, we assessed the absolute strength of the memory by conducting a probe trial, which replaced the first RT. In these probe trials, the previously rewarded sandwell did not contain reward for the first minute of exploration (Videos S2 and S3). The initial absence of reward did not discourage the mouse from revisiting the rewarded arm during the probe trial (Figure S2H). Memory in probe trials was quantified as the relative dig time at the rewarded sandwell, normalized to the total dig time at the rewarded and non-rewarded sandwells (termed the "occupancy difference score"). In sessions conducted with spaced encoding intertrial intervals, we observed an inverted U-shaped effect of trial spacing on next-day memory. Specifically, mice that were trained using a 10- or 180-min encoding intertrial interval did not remember the rewarded location after 24 h (Figures 1F and S2I), whereas memories persisted after training with encoding intertrial intervals of 30 or 60 min (Figure 1F). Unexpectedly, massed training did not result in same-day memory, but memory was observed after 24 h and was even still present after 48 h (see Discussion; Figures 1F and S2I).

Differences in trial spacing could affect a number of memory-related behavioral variables besides error-based performance: latency to find the rewarded sandwell, distance traveled, running speed, relative dig time, and number of arm visits (Figure S3). In consecutive ETs, we observed a quantitative reduction in the variables that are indicative of exploration, i.e., latency, distance traveled, running speed, and number of arms visited. Conversely, we observed an increase in the relative dig time, a measure of exploitation of memory of the rewarded location. These results suggest that mice explored less and increasingly used their recollection of the rewarded sandwell location in subsequent ETs. Some behavioral

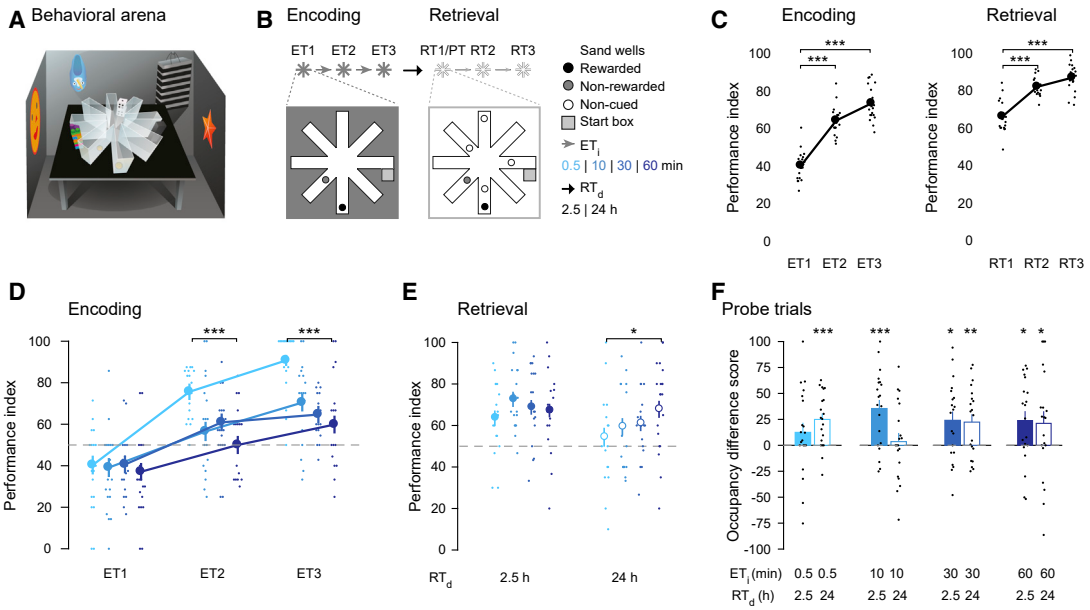

Figure 1. Trial spacing enhances memory retrieval yet impairs memory encoding in the everyday memory task

(A) Schematic of the behavioral training setup.

(B) Schematic of the session structure. Each session consisted of a learning phase ("encoding", three trials separated by an "encoding intertrial interval" [ET_i]) and a memory phase ("retrieval", three trials), separated by a retrieval delay (RT_d). Occasionally, the first retrieval trial (RT1) was replaced with a probe trial (PT, no reward present for the first 60 s). The location of the sandwells and start box was altered on each session.

(C) Performance improved across ETs and RTs (one-way repeated-measures [OWRM] ANOVA: $F_{5,90} = 110.5$, $p = 7.24 \cdot 10^{-37}$; Bonferroni post hoc tests: ET1 versus ET2, $p = 1.22 \cdot 10^{-9}$; ET1 versus ET3, $p = 2.27 \cdot 10^{-8}$; RT1 versus RT2, $p = 1.10 \cdot 10^{-5}$; RT1 versus RT3, $p = 3.00 \cdot 10^{-6}$; n = 19 mice).

(D) Performance increased on subsequent ETs but was generally lower for longer ET_is (two-way repeated-measures [TWRM] ANOVA: trial number, $F_{2,108} = 111$, $p = 1.17 \cdot 10^{-15}$; ET_i, $F_{3,108} = 11.7$, $p = 6.00 \cdot 10^{-6}$; interaction, $F_{6,108} = 2.50$, $p = 0.027$; Bonferroni post hoc tests: 0.5 versus 10 min, $p = 0.003$; 0.5 versus 30 min, $p = 0.004$; 0.5 versus 60 min, $p = 9.30 \cdot 10^{-5}$; ET1 versus ET2, $p = 3.87 \cdot 10^{-10}$; ET1 versus ET3, $p = 6.37 \cdot 10^{-9}$; ET2 versus ET3, $p = 2.88 \cdot 10^{-4}$; n = 19 mice).

(E) Increasing the ET_i did not alter performance in RT1 after a 2.5-h RT_d (OWRM ANOVA: $F_{3,54} = 1.58$, $p = 0.206$; n = 19 mice) yet did after 24 h (OWRM ANOVA: $F_{3,54} = 3.02$, $p = 0.038$; n = 19 mice).

(F) Memory expression in probe trials was not observed after 2.5 h if training was conducted with an ET_i of 0.5 min, but was after 24 h (one-sample t test: RT_d 2.5 h versus chance, $t_{18} = 1.35$, $p = 0.194$; RT_d 24 h versus chance, $t_{18} = 4.27$, $p = 4.12 \cdot 10^{-4}$; n = 19 mice). Conversely, training with an ET_i of 10 min resulted in memory after 2.5 h but not after 24 h (one-sample t test: RT_d 2.5 h versus chance, $t_{18} = 4.30$, $p = 3.89 \cdot 10^{-4}$; RT_d 24 h versus chance, $t_{18} = 0.43$, $p = 0.675$; n = 19 mice). Memory was present and stable on probe trials conducted after training using a 30- or 60-min ET_i (one-sample t test: ET_i 30 min; RT_d 2.5 h versus chance, $t_{18} = 2.83$, $p = 0.011$; RT_d 24 h versus chance, $t_{18} = 2.94$, $p = 0.008$; ET_i 60 min; RT_d 2.5 h versus chance, $t_{18} = 2.63$, $p = 0.017$; RT_d 24 h versus chance: $t_{18} = 2.48$, $p = 0.023$; n = 19 mice).

Filled dots indicate data from one mouse, circles and bars indicate mean (±SEM) across mice, and gray dashed lines indicate chance level. *$p < 0.05$, **$p < 0.01$, ***$p < 0.001$. See also Figures S1–S3 and Videos S1, S2, and S3.

variables showed also a significant effect for trial spacing (Figure S3). However, these effects were restricted to specific trial conditions (i.e., only a single ET, RT, encoding intertrial interval, or retrieval delay) and did not follow a systematic pattern, thus indicating that there was no general effect of trial spacing on these variables. We conclude that increased trial spacing enhances memory retrieval, independent of the impairing effect on memory encoding.

The dmPFC is activated and necessary during the everyday memory task

To validate that training in the everyday memory task activates the dmPFC, we quantified neuronal activation resulting from training on the three ETs using expression of the immediate-early gene c-Fos (Figure 2A). c-Fos expression in the dmPFC was increased after training as compared to handled or home cage controls (Figures 2B and 2C). However, the number of c-Fos-expressing neurons was similar after training spaced with any encoding intertrial interval. This suggests that trial spacing did not increase the number of activated neurons during memory encoding.

To establish a causal role of the dmPFC in the everyday memory task, we performed experiments while chemogenetically inhibiting this region. We bilaterally transduced excitatory dmPFC neurons with the inhibitory chemogenetic tool hM4D(Gi), which is activated by clozapine-*N*-oxide (CNO; Figures 3A and 3B).[34] Post hoc analysis of fixed brain tissue confirmed robust bilateral expression of the viral vector, with some inter-animal variability in dmPFC subregions (data not shown). We verified receptor function in dmPFC *ex vivo* electrophysiological recordings, establishing that CNO application to acute brain slices reduced the excitability of dmPFC neurons expressing the DREADD (designer receptor exclusively activated by designer drugs) hM4D(Gi) (Figures S4A–S4C).

The role of dmPFC activity in the everyday memory task was assessed in well-trained mice, using a 2^4 factorial design. Mice

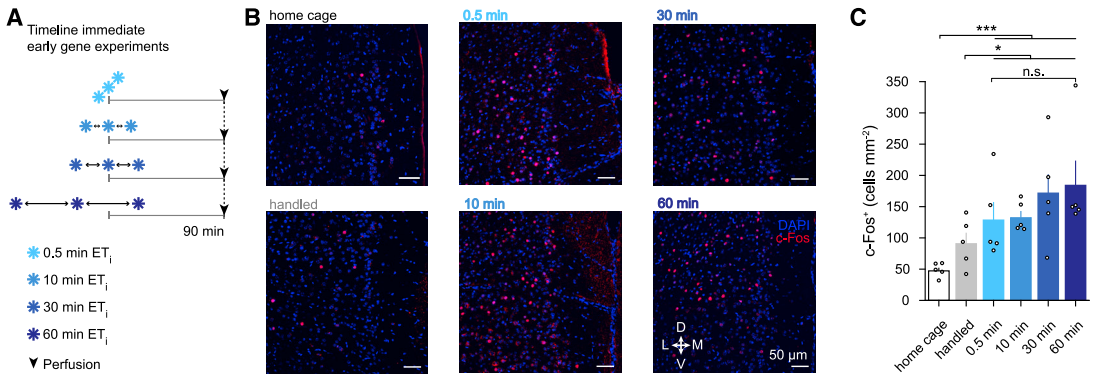

Figure 2. The dmPFC is activated by training on the everyday memory task, irrespective of trial spacing

(A) Timeline of behavioral procedures and tissue collection. Horizontal lines denote time.

(B) Representative intensity adjusted images of c-Fos labeling in the dmPFC.

(C) Training with any ET_i increased the number of cells expressing c-Fos as compared to home cage or handled controls (Kruskal-Wallis test: $H_2 = 15.8$, $p = 3.65 \cdot 10^{-4}$; Mann-Whitney U post hoc tests: training versus home cage, $U = 0$, $p = 7.71 \cdot 10^{-4}$; training versus handled, $U = 19$, $p = 0.013$; $n = 5$ mice per group). Increasing the ET_i did not alter the number of c-Fos-expressing cells (Kruskal-Wallis test: $H_3 = 1.19$, $p = 0.754$; $n = 5$ mice per group).

Scale bars represent 50 µm. Bars indicate mean (±SEM) across mice; dots indicate data from a single mouse. *$p < 0.05$, ***$p < 0.001$; n.s., non-significant.

expressing either hM4D(Gi) (n = 7) or mCherry (n = 5; genotype) were injected with either vehicle or CNO (drug) at either of two time points (before memory encoding or before retrieval), using either of two encoding intertrial intervals (0.5 or 60 min; see STAR Methods). First, we tested the main hypothesis that dmPFC inactivation affects memory performance in general, that is, whether CNO injection in hM4D(Gi)-expressing mice reduced their ability to remember the location of the rewarded sandwell. To this end, we averaged the data per mouse over the injection time points and encoding intertrial intervals, resulting in four groups: mCherry-vehicle, mCherry-CNO, hM4D(Gi)-vehicle, and hM4D(Gi)-CNO. All three comparisons of hM4D(Gi)-expressing, CNO-injected mice with the vehicle-injected and mCherry-expressing control groups showed that mice in which the dmPFC was inactivated performed significantly poorer in the task (Figure 3C).

Subsequently, we assessed memory performance in more detail, testing all experimental factors, genotype, drug, time point, and encoding intertrial interval, as well as their interactions, using a four-way ANOVA. Although this analysis indicated an effect of genotype and drug, it did not reveal any effects of other factors (time point, encoding intertrial interval) or their interactions on memory performance (Figure 3D). We note that the relatively low number of subjects in this part of the study increased the risk of a type II error (false negative), especially for the four-way full-factorial ANOVA. In summary, we conclude that chemogenetic inactivation of the dmPFC generally impairs memory performance in the everyday memory task and we did not find evidence suggesting a specific role of dmPFC activity at individual injection time points or encoding intertrial intervals.

Trial spacing increases the stability of the dmPFC activation pattern

The major aim of this study was to evaluate whether trial spacing stabilizes the activity patterns of the neuronal populations throughout a session, i.e., whether it facilitates reactivation of a similar neuronal ensemble in subsequent trials. To this end, we used *in vivo* calcium imaging to simultaneously measure the activity patterns of on average 210 ± 99 (SD) individual dmPFC neurons per session in freely moving mice (n = 499 sessions across 19 mice). After gaining optical access to the dmPFC with an implanted microprism, we used a miniaturized microscope to image neurons expressing the calcium indicator GCaMP6m (see STAR Methods; Figures 4A–4C and S4D–S4H).[35,36] We ensured that carrying the miniaturized microscope did not hamper the mouse's motility in the radial arm maze (Figures S4I and S4J). Using the constrained nonnegative matrix factorization for microendoscopic data (CNMF-E) algorithm,[37] we extracted neuronal calcium activity and used the deconvolved inferred spike rate for further analysis (see STAR Methods; Figure S5). The total number of identified neurons (CNMF-E sources) did not vary between experimental conditions (Figure S6A). We computed the probability of a neuron being active by comparing the inferred spike rate in each trial to the pre-trial baseline period, using temporal subsampling to control for session duration (p_{active}; see STAR Methods; Figures S6B–S6D). The average p_{active} was similar in the dorsal and ventral halves of the field of view across sessions, suggesting homogeneous activity across the dmPFC. We subsequently concatenated these values into an ensemble response vector and stacked the single-trial ensemble response vectors into an ensemble response matrix (n neurons × 6 trials; Figure 4D). The Pearson correlation between the rows of this matrix was used as the session's trial-to-trial ensemble stability measure (Figure 4D).

The ensemble correlation between the first and second ETs was enhanced when the intertrial interval was longer, establishing that the ensemble reactivated more precisely (Figures 4E and 4F). Furthermore, trial spacing increased the ensemble correlation between the third ET and the first RT, suggesting that the population activity pattern present during learning was more likely to be reactivated during retrieval (Figures 4E and 4F). The effect of trial spacing on ensemble correlation was not dependent on behavioral performance. As an alternative measure for similarity, we calculated the Euclidian distance between ensemble response vectors, which yielded similar results (Figure S6E). Overall, we find that increased trial spacing enhanced

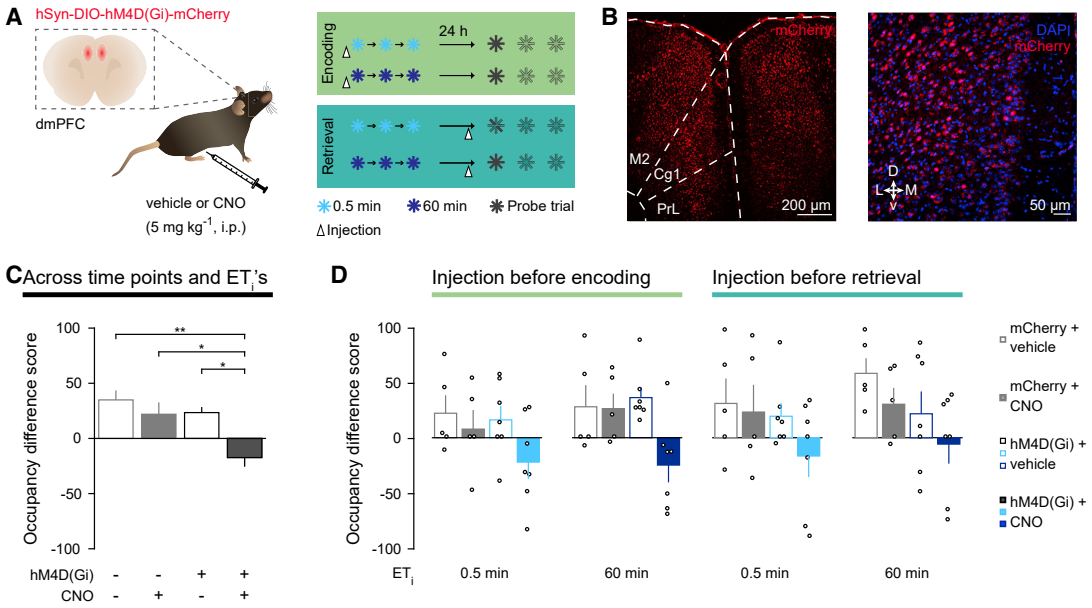

Figure 3. Chemogenetic inactivation of the dmPFC impairs task-related memory

(A) Chemogenetic silencing experiment. After bilateral transduction of the dmPFC with either mCherry (n = 5 mice) or hM4D(Gi) (n = 7 mice), mice were injected with vehicle or CNO during a subset of behavioral experiments.

(B) Representative intensity adjusted images of hM4D(Gi)-mCherry-expressing neurons in the dmPFC.

(C) On probe trials, memory performance of CNO-injected, hM4D(Gi)-expressing mice was reduced in comparison to the three control groups (independent-samples t test: versus mCherry-CNO, $t_{10} = 2.97$, $p = 0.014$; versus mCherry-vehicle, $t_{10} = 4.31$, $p = 0.002$; paired-samples t test: versus hM4D(Gi)-vehicle, $t_6 = -3.73$, $p = 0.010$; $n_{hM4D(Gi)} = 7$ mice, $n_{mCherry} = 5$ mice).

(D) Memory performance, as in (C), but separated for all experimental groups in the 2^4 factorial design (see A). Left block: experiments in which CNO or vehicle was injected before the encoding session. Right block: as on the left, but with the injection before the retrieval session. Per block: left: massed training, ET_i 0.5 min; right: spaced training, ET_i 60 min. Memory performance was not affected by any other factors than drug and genotype (four-way mixed-design [FWMD] ANOVA: drug, $F_{1,10} = 9.08$, $p = 0.013$; genotype, $F_{1,10} = 12.52$, $p = 0.005$; all other main effects and interactions, $p > 0.05$; $n_{hM4D(Gi)} = 7$ mice, $n_{mCherry} = 5$ mice).

Cg1, cingulate cortex, area 1; M2, secondary motor cortex; PrL, prelimbic cortex. Scale bars represent 200 μm (B, left) and 50 μm (B, right). Bars indicate mean (±SEM) across mice; dots indicate data from a single mouse. *$p < 0.05$, **$p < 0.01$; n.s., non-significant. See also Figure S4.

reactivation of the ensemble activity pattern instilled during encoding, while simultaneously strengthening memory retention.

The size of the neuronal ensemble is not affected by trial spacing

We evaluated whether trial spacing altered the size of the neuronal ensemble (Figure 5A). From the cumulative distribution of each trial's ensemble response vector, we inferred the active fraction within the neuronal population (i.e., the neuronal ensemble, $p_{active} > 0$) and the median activity of that population (Figure 5A). Interestingly, the neuronal ensembles became smaller across subsequent ETs and RTs (i.e., first versus second versus third trial; Figure 5B). In addition, the median activity of the neuronal ensemble increased across subsequent trials (Figure 5B), indicating that the ensemble became sparser yet the single neurons responded more strongly (see Discussion). However, neither ensemble size (i.e., the relative number of active neurons) nor its median activity was altered by trial spacing (Figure 5B).

With the overall ensemble size remaining stable, the memory-enhancing effect of trial spacing could be attributed to a shift in the fraction of neurons preferentially responding to task-related events. We identified eight task-related behavioral variables that correlated with reward, motor activity, and decision making: reward onset, reward approach (i.e., the final entry into the arm containing the rewarded sandwell), acceleration, speed, digging onset, digging offset, entry into the center platform, and intra-arm turns. On first inspection, neuronal responses did not appear time locked or consistently occurring with the onset of these defined behaviors (Figure S5E). This was likely related to the naturalistic character of the everyday memory task, in which the individual components that comprise a behavior can occur simultaneously, whereas these appear discrete in more controlled experimental settings.

To determine whether the activity of individual neurons was modulated by task-relevant behaviors, we implemented an encoding model (generalized linear model; GLM). The model fitted the eight aforementioned behavioral variables as time-varying predictors of a neuron's binarized inferred firing activity (see STAR Methods; Figures 6A and 6B).[38] A neuron was classified as responsive to one of these behavioral variables if the weight of its corresponding time-varying predictor was significantly different from zero. Decoding performance was better upon training the encoding model with observed as compared to permuted inferred firing activity (Figure 6C). Across sessions, 22.7% of neurons were significantly modulated by at least one behavioral variable, most often reward onset, approach to reward, and digging onset (19.9%,

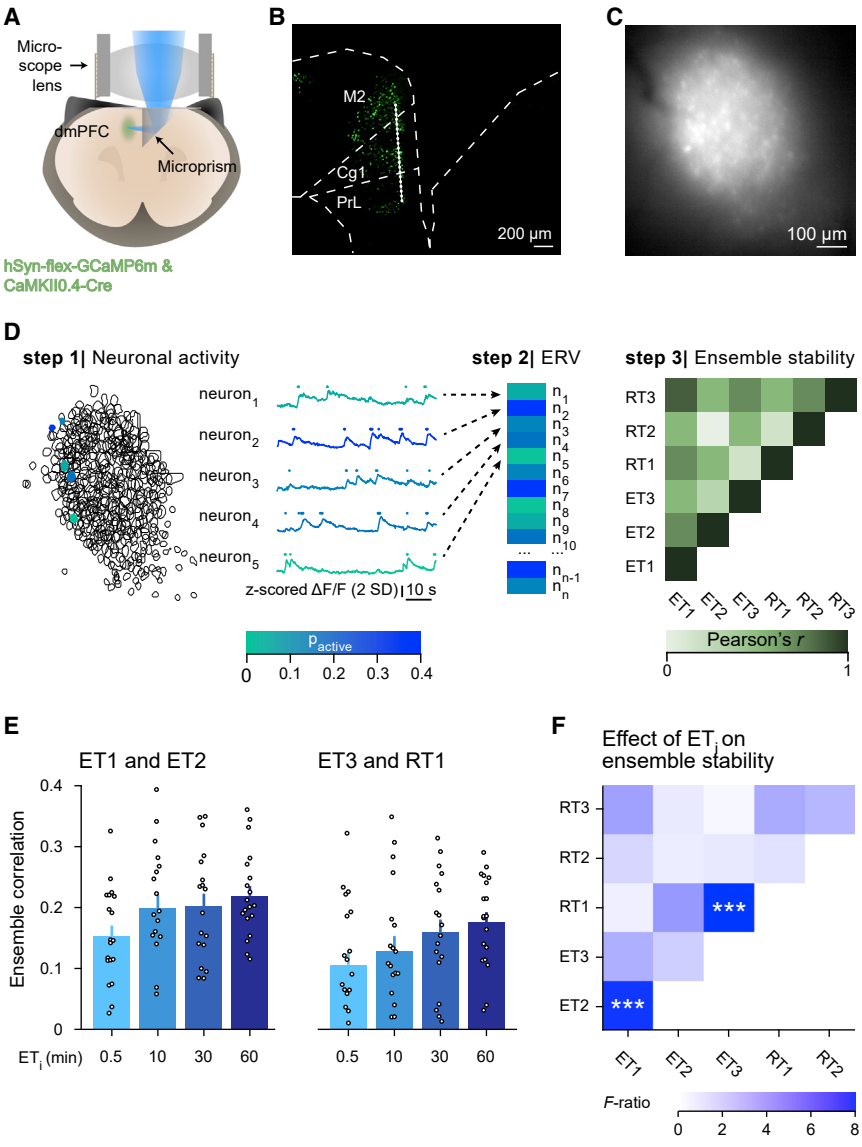

Figure 4. Trial spacing enhances ensemble stability

(A) Schematic of the imaging preparation.

(B) Coronal section of the dmPFC showing GCaMP6m expression and the approximate imaging plane (dotted line).

(C) Example single imaging frame acquired with the miniature microscope.

(D) Schematic showing the quantification of ensemble stability. Based on the deconvolved spiking activity (dots, calcium activity displayed as traces), the activity measure "p_{active}" was calculated for each neuron (see color code for p_{active} of example neurons in the field of view; step 1). The p_{active} of individual neurons was concatenated into an ensemble response vector for each trial (ERV; step 2). The correlation between ensemble response vectors of a session was used as a measure for ensemble stability (step 3).

(E) Ensemble correlation between ET1 and ET2 (left) and between ET3 and RT1 (right).

(F) Trial spacing enhanced the ensemble correlation between ET1 and ET2, as well as between ET3 and RT1 (OWRM ANOVA: ET1–ET2, $F_{3,54} = 6.98$, $p = 5.07 \cdot 10^{-4}$; Bonferroni post hoc tests: 0.5 versus 10 min, $p = 3.16 \cdot 10^{-4}$; 0.5 versus 60 min, $p = 2.04 \cdot 10^{-3}$; ET3–RT1, $F_{3,54} = 7.28$ $p = 3.72 \cdot 10^{-4}$; Bonferroni post hoc tests: 0.5 versus 30 min, $p = 2.56 \cdot 10^{-3}$; 0.5 versus 60 min, $p = 1.51 \cdot 10^{-3}$; n = 19 mice).

SD, standard deviation. Scale bars represent 200 µm (B) and 100 µm (C). Bars indicate mean (±SEM) across mice; dots indicate data from a single mouse, averaged across sessions. ***p < 0.001. See also Figures S4–S6.

16.2%, and 18.1% of the population of modulated neurons, respectively; Figure 6D). This shows that dmPFC neuronal activity during the everyday memory task is modulated by specific behavioral variables.

However, trial spacing did not have a significant influence on the fractions of behaviorally modulated neurons, nor did the encoding performance or retrieval delay duration (Figure 6E). Firing modulation by all identified task-relevant behaviors did depend on session duration (Figure 6E), likely because an increased session duration inherently produces more neuronal spikes and therefore data for the GLM to fit. Furthermore, retrieval performance correlated with the fraction of neurons modulated by certain behavioral variables, i.e., running speed, reward approach, dig onset, dig offset, entry into the center platform, and intra-arm turns. Therefore, we conclude that a sparse population of dmPFC neurons encoded task-related behaviors similarly across experimental conditions and we did not find evidence of an effect of trial spacing on the number of neurons involved.

Overall, trial spacing in the everyday memory task enhances ensemble stability but it does not affect ensemble size.

DISCUSSION

We explored whether trial spacing strengthens memory by altering characteristics of the neuronal ensemble. We observed the behavioral effect of trial spacing on the everyday memory task and characterized the activity of prefrontal neurons that were necessary for task performance. During learning and upon memory retrieval, the ensemble activity pattern reactivated more precisely when trial spacing was increased. In contrast, trial spacing did not affect the overall size of the activated ensemble, nor the size of the subpopulations of neurons that responded to specific task-related behaviors. Our results suggest that more precise reactivation of the neuronal ensemble during spaced training strengthens connectivity that is conducive to memory retention and retrieval.

Spaced training strengthens memory

Spaced training in the everyday memory task strengthens memory in rats[7] and we report the same in mice. Earlier studies investigating the effect of trial spacing on episodic-like memory in mice[6] and rats[39] have reported an inverted U-shaped relation,

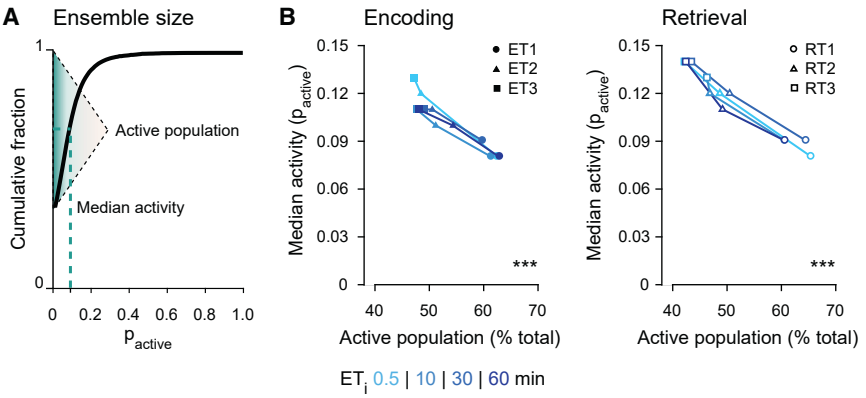

Figure 5. Trial spacing does not affect the size of the complete neuronal ensemble

(A) Schematic showing the quantification of ensemble size. The sizes of the active population ($p_{active} > 0$) and its median activity were inferred from the cumulative distribution of the ensemble response vector.

(B) The trial identity (i.e., first, second, or third trial) but not the ET_i affected the size of the active population (TWRM ANOVA: trial identity, $F_{5,270} = 61.4$, $p = 9.15 \cdot 10^{-27}$; ET_i, $F_{3,270} = 2.28$, $p = 0.091$; Bonferroni post hoc tests for subsequent trials: ET1 versus ET2, $p = 1.00 \cdot 10^{-6}$; RT1 versus RT2, $p = 6.80 \cdot 10^{-8}$; n = 19 mice) and its median activity (TWRM ANOVA: trial identity, $F_{5,270} = 91.7$, $p = 9.57 \cdot 10^{-33}$; ET_i; $F_{3,270} = 2.10$, $p = 0.111$; Bonferroni post hoc tests for subsequent trials: ET1 versus ET2, $p = 3.12 \cdot 10^{-8}$; RT1 versus RT2, $p = 9.90 \cdot 10^{-7}$; RT2 versus RT3, $p = 0.004$; n = 19 mice) during both encoding (left) and retrieval (right).

Data points indicate the mean across mice. ***$p < 0.001$.

although the exact width and amplitude of the effect varied. Our study likewise reports an inverted U-shaped relation, as spacing trials at intervals of 60 min resulted in the strongest next-day (24-h) memory, whereas shorter (10 and 30 min) and longer intervals (180 min) resulted in substantially poorer memory. The observed temporal window aligns with expectations from facilitated molecular signaling and synaptic physiology underlying the spacing effect.[2,6,8]

As compared to spaced training, massed training in the everyday memory task affected memory in a rather complex manner. As expected, memory retrieval was poorer after massed training than after any spaced training regimen. Surprisingly, the ability to retrieve memory following massed training was better after 24 h, and even 48 h, as compared to 2.5 h. We propose that memory acquired during massed training might have only been stabilized after several hours. A similar phenomenon has been reported during massed motor learning in mice, in which both memory stabilization and concomitant synaptic remodeling occurred delayed as compared to spaced motor learning.[5] However, delayed memory stabilization was not observed in two earlier studies using the everyday memory task.[7,40] This variation can possibly be attributed to methodological differences such as the animal model,[7,40] number of ETs,[40] navigational strategy,[33] handling, or intertrial sleep epochs.

Prefrontal activity in the everyday memory task

We focused our neuronal recordings and manipulations on the dmPFC. Activity of dmPFC neurons correlated with a range of task-relevant events on the everyday memory task, most notably reward (anticipation) and motor behavior, which is consistent with other reports in rodent PFC.[41,42] By chemogenetically inactivating the dmPFC, we provide evidence for a causal link between dmPFC activity and performance in the everyday memory task. Beyond this general effect, we were unable to determine whether memory performance was especially affected by dmPFC inactivation during massed or spaced learning, or during encoding or retrieval. The finding of a link between dmPFC inactivation and impaired next-day memory seemingly conflicts with reports that inactivation of prefrontal areas disrupts remote but not recent memories.[43] However, the early dependence of task-instilled memories on the dmPFC may have followed from accelerated systems consolidation, as observed in other behavioral paradigms where learning occurred within the context of relevant pre-existing knowledge.[30]

Episodic-like memories formed in the everyday memory task unlikely depended solely on the dmPFC. Specifically the hippocampus[44] and retrosplenial cortex[45] have long been implicated in various forms of declarative memory. Indeed, the hippocampus and PFC have been suggested to perform complementary roles in episodic-like memory processing.[31,46] Furthermore, retrosplenial neurons form ensembles that stabilize during learning of spatial reference memory tasks[47] and the stability of these retrosplenial ensembles can predict memory retention.[48] Interestingly, a recent study shows that trial spacing upregulates a variety of genes, including immediate-early genes, in both the hippocampus and retrosplenial cortex in the rat.[7] Whether and how neuronal ensembles in the mouse hippocampus and retrosplenial cortex are affected by spaced training in the everyday memory task would be of interest for future investigation.

The spacing effect, synaptic strength, and memory stability

Our experiments explored the possibility that trial spacing enhances memory by altering the size or stability of a neuronal ensemble. We quantified ensemble size using two distinct methods. First, we determined the neuronal ensemble size using calcium imaging of GCaMP6-expressing neurons, which closely reflects the temporal dynamics of neuronal firing throughout each trial.[36] This approach allowed for detecting both highly active and transiently activated neurons, while controlling for the influence of training duration on ensemble size by temporal subsampling. Second, we quantified ensemble size from the number of c-Fos-expressing neurons after a full encoding session. This method is more likely to only include strongly activated neurons that subsequently underwent plasticity implicated in long-term memory storage.[49] Despite the methodological differences between these approaches, both yielded similar results: the size of the active population was not influenced by trial spacing. This is in agreement with the previous observation that ensemble size is generally quite stable and is not strongly

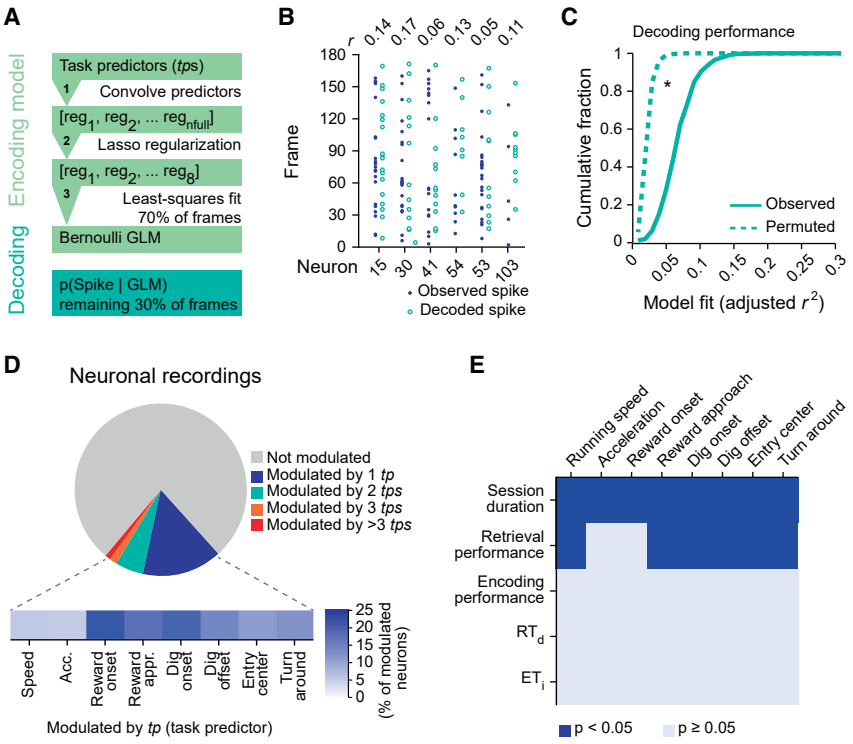

Figure 6. dmPFC neurons respond to multiple task-relevant behaviors irrespective of trial spacing

(A) Schematic of the GLM to identify neurons whose firing was modulated by specific task-related behaviors and events.

(B) Pearson's r between observed and decoded spikes of the test subset for six randomly selected neurons.

(C) Decoding performance was significantly better for observed than permuted spiking activity (Kolmogorov-Smirnov test: observed versus permuted, $D_{100} = 0.21$, $p = 0.021$; n = 499 sessions).

(D) Fractions of neurons (n = 105,070 neurons from 499 sessions across 19 mice) that were modulated (top). Fractions of neurons modulated by the respective task predictor (bottom).

(E) The effect of the five features, session duration, performance in RT1 ("retrieval performance"), summed performance across ETs ("encoding performance"), encoding intertrial interval (ET_i), and RT_d, on the fraction of neurons modulated by the eight *tps*. These five features differentially affected the fraction of neurons modulated by running speed (FW ANOVA: session duration [SeD], $F = 121$, $p = 2.95 \cdot 10^{-25}$; retrieval performance [RP], $F_{5,810} = 3.05$, $p = 0.01$; n = 499 sessions), acceleration (FW ANOVA: SeD, $F = 76.6$, $p = 3.43 \cdot 10^{-17}$; n = 499 sessions), reward onset (FW ANOVA: SeD, $F = 67.7$, $p = 1.78 \cdot 10^{-15}$; n = 499 sessions), reward approach (FW ANOVA: SeD, $F = 86.8$, $p = 4.14 \cdot 10^{-19}$; RP, $F_{5,810} = 6.37$, $p = 1.00 \cdot 10^{-5}$; n = 499 sessions), dig onset (FW ANOVA: SeD, $F = 121$, $p = 2.42 \cdot 10^{-25}$; RP, $F_{5,810} = 2.89$, $p = 0.014$; n = 499 sessions), dig offset (FW ANOVA: SeD, $F = 129$, $p = 1.31 \cdot 10^{-26}$; RP, $F_{5,810} = 3.18$, $p = 0.008$; n = 499 sessions), entry into the center platform (FW ANOVA: SeD, $F = 108$, $p = 5.89 \cdot 10^{-23}$; RP, $F_{5,810} = 7.74$, $p = 5.10 \cdot 10^{-7}$; n = 499 sessions), and intra-arm turns (FW ANOVA: SeD, $F = 86.8$, $p = 4.14 \cdot 10^{-19}$; RP, $F_{5,810} = 4.36$, $p = 6.78 \cdot 10^{-4}$; n = 499 sessions). Only significant tests are reported.

Acc, acceleration; appr, approach; GLM, generalized linear model; *tp*, task predictor; reg, regressor. *p < 0.05. See also Figure S5.

influenced by factors such as the type of memory and the strength of a memory.[24]

Irrespective of trial spacing, behavioral training activated a progressively smaller population of neurons, whose activity was stronger than in previous trials. Sparsening of the neuronal ensemble can enhance memory selectivity, as for instance observed during *Drosophila* olfactory conditioning.[26] Several studies propose that this is the consequence of a competitive process,[9,24] in which highly excitable pyramidal neurons exclude less excitable neighboring pyramidal neurons from becoming part of the neuronal ensemble via local inhibition. A similar process might ensure ensemble sparsity in the everyday memory task, thereby balancing memory fidelity with memory capacity.[9]

The main consequence of trial spacing was that the neuronal ensemble reactivated in a pattern more reminiscent of previous learning experiences, corroborating theoretical predictions[50] and reports in human subjects.[23] Yet, the question of whether the enhanced stability of the ensemble pattern is causal for the memory-enhancing effect of trial spacing remains so far unanswered. We suggest that more precise ensemble reactivation reflects specific synaptic processes that underlie memory formation.[15] One such process is Ca^{2+}/calmodulin-dependent protein kinase II (CaMKII) activation, which unfolds on a similar timescale as spacing-induced memory enhancement and has previously been implicated in the spacing effect.[2] A major outstanding question is whether these synaptic processes affect a random population of synapses or are confined to previously tagged synapses, as predicted by the synaptic tagging and capture hypothesis.[51] This could be addressed using *in vivo* imaging of structure and function of individual spines during the everyday memory assay.[52]

Overall, our data show that trial spacing increases the strength of connectivity within the ensemble, supposedly making memory more robust and increasing the probability of memory retrieval. Our findings provide the first direct description of how activity of the same neuronal population during memory encoding and retrieval mediates the spacing effect, a phenomenon originally described over a century ago.[1]

STAR★METHODS

Detailed methods are provided in the online version of this paper and include the following:

- KEY RESOURCES TABLE
- RESOURCE AVAILABILITY
  - Lead contact
  - Materials availability
  - Data and code availability
- EXPERIMENTAL MODEL AND SUBJECT DETAILS
- METHOD DETAILS
  - Surgical procedures

SUPPLEMENTAL INFORMATION

Supplemental information can be found online at https://doi.org/10.1016/j.cub.2021.06.085.

ACKNOWLEDGMENTS

We thank Claudia Huber, Andreas Kucher, Max Sperling, Volker Staiger, Helena Tultschin, and Frank Voss for technical assistance; Sandra Reinert for help with the implant method and discussions; and Julia Kuhl for illustrations. This project was funded by the Max Planck Society and Collaborative Research Center SFB870 (project numbers A07 and A08; reference number 118803580) of the German Research Foundation (DFG) (to T.B. and M.H.).

AUTHOR CONTRIBUTIONS

All authors designed the study. A.G. acquired the data. A.G. and P.M.G. analyzed the data. T.B. and M.H. acquired funding. All authors wrote the manuscript.

DECLARATION OF INTERESTS

The authors declare no competing interests.

Received: December 15, 2020
Revised: June 1, 2021
Accepted: June 28, 2021
Published: July 28, 2021

REFERENCES

1. Ebbinghaus, H. (1885). Über das Gedächtnis: Untersuchungen zur Experimentellen Psychologie (Duncker & Humblot).
2. Smolen, P., Zhang, Y., and Byrne, J.H. (2016). The right time to learn: mechanisms and optimization of spaced learning. Nat. Rev. Neurosci. *17*, 77–88.
3. Kogan, J.H., Frankland, P.W., Blendy, J.A., Coblentz, J., Marowitz, Z., Schütz, G., and Silva, A.J. (1997). Spaced training induces normal long-term memory in CREB mutant mice. Curr. Biol. *7*, 1–11.
4. Genoux, D., Haditsch, U., Knobloch, M., Michalon, A., Storm, D., and Mansuy, I.M. (2002). Protein phosphatase 1 is a molecular constraint on learning and memory. Nature *418*, 970–975.
5. Aziz, W., Wang, W., Kesaf, S., Mohamed, A.A., Fukazawa, Y., and Shigemoto, R. (2014). Distinct kinetics of synaptic structural plasticity, memory formation, and memory decay in massed and spaced learning. Proc. Natl. Acad. Sci. USA *111*, E194–E202.
6. Seese, R.R., Wang, K., Yao, Y.Q., Lynch, G., and Gall, C.M. (2014). Spaced training rescues memory and ERK1/2 signaling in fragile X syndrome model mice. Proc. Natl. Acad. Sci. USA *111*, 16907–16912.
7. Nonaka, M., Fitzpatrick, R., Lapira, J., Wheeler, D., Spooner, P.A., Corcoles-Parada, M., Muñoz-López, M., Tully, T., Peters, M., and Morris, R.G.M. (2017). Everyday memory: towards a translationally effective method of modelling the encoding, forgetting and enhancement of memory. Eur. J. Neurosci. *46*, 1937–1953.
8. Kramár, E.A., Babayan, A.H., Gavin, C.F., Cox, C.D., Jafari, M., Gall, C.M., Rumbaugh, G., and Lynch, G. (2012). Synaptic evidence for the efficacy of spaced learning. Proc. Natl. Acad. Sci. USA *109*, 5121–5126.
9. Rao-Ruiz, P., Yu, J., Kushner, S.A., and Josselyn, S.A. (2019). Neuronal competition: microcircuit mechanisms define the sparsity of the engram. Curr. Opin. Neurobiol. *54*, 163–170.
10. Silva, A.J., Zhou, Y., Rogerson, T., Shobe, J., and Balaji, J. (2009). Molecular and cellular approaches to memory allocation in neural circuits. Science *326*, 391–395.
11. Garner, A.R., Rowland, D.C., Hwang, S.Y., Baumgaertel, K., Roth, B.L., Kentros, C., and Mayford, M. (2012). Generation of a synthetic memory trace. Science *335*, 1513–1516.
12. Rashid, A.J., Yan, C., Mercaldo, V., Hsiang, H.L., Park, S., Cole, C.J., De Cristofaro, A., Yu, J., Ramakrishnan, C., Lee, S.Y., et al. (2016). Competition between engrams influences fear memory formation and recall. Science *353*, 383–387.
13. Hebb, D.O. (1949). The Organization of Behavior: A Neuropsychological Theory (Wiley).
14. Engert, F., and Bonhoeffer, T. (1999). Dendritic spine changes associated with hippocampal long-term synaptic plasticity. Nature *399*, 66–70.
15. Holtmaat, A., and Caroni, P. (2016). Functional and structural underpinnings of neuronal assembly formation in learning. Nat. Neurosci. *19*, 1553–1562.
16. Nadel, L., and Moscovitch, M. (1997). Memory consolidation, retrograde amnesia and the hippocampal complex. Curr. Opin. Neurobiol. *7*, 217–227.
17. Tonegawa, S., Morrissey, M.D., and Kitamura, T. (2018). The role of engram cells in the systems consolidation of memory. Nat. Rev. Neurosci. *19*, 485–498.
18. Liu, X., Ramirez, S., Pang, P.T., Puryear, C.B., Govindarajan, A., Deisseroth, K., and Tonegawa, S. (2012). Optogenetic stimulation of a hippocampal engram activates fear memory recall. Nature *484*, 381–385.
19. Reijmers, L.G., Perkins, B.L., Matsuo, N., and Mayford, M. (2007). Localization of a stable neural correlate of associative memory. Science *317*, 1230–1233.
20. Pignatelli, M., Ryan, T.J., Roy, D.S., Lovett, C., Smith, L.M., Muralidhar, S., and Tonegawa, S. (2019). Engram cell excitability state determines the efficacy of memory retrieval. Neuron *101*, 274–284.e5.
21. Kitamura, T., Ogawa, S.K., Roy, D.S., Okuyama, T., Morrissey, M.D., Smith, L.M., Redondo, R.L., and Tonegawa, S. (2017). Engrams and circuits crucial for systems consolidation of a memory. Science *356*, 73–78.
22. Choi, J.-H., Sim, S.-E., Kim, J.-I., Choi, D.I., Oh, J., Ye, S., Lee, J., Kim, T., Ko, H.-G., Lim, C.S., and Kaang, B.K. (2018). Interregional synaptic maps among engram cells underlie memory formation. Science *360*, 430–435.
23. Feng, K., Zhao, X., Liu, J., Cai, Y., Ye, Z., Chen, C., and Xue, G. (2019). Spaced learning enhances episodic memory by increasing neural pattern similarity across repetitions. J. Neurosci. *39*, 5351–5360.
24. Morrison, D.J., Rashid, A.J., Yiu, A.P., Yan, C., Frankland, P.W., and Josselyn, S.A. (2016). Parvalbumin interneurons constrain the size of the lateral amygdala engram. Neurobiol. Learn. Mem. *135*, 91–99.
25. Gdalyahu, A., Tring, E., Polack, P.O., Gruver, R., Golshani, P., Fanselow, M.S., Silva, A.J., and Trachtenberg, J.T. (2012). Associative fear learning enhances sparse network coding in primary sensory cortex. Neuron *75*, 121–132.
26. Lin, A.C., Bygrave, A.M., de Calignon, A., Lee, T., and Miesenböck, G. (2014). Sparse, decorrelated odor coding in the mushroom body enhances learned odor discrimination. Nat. Neurosci. *17*, 559–568.
27. Vyazovskiy, V.V., Cirelli, C., Pfister-Genskow, M., Faraguna, U., and Tononi, G. (2008). Molecular and electrophysiological evidence for net

synaptic potentiation in wake and depression in sleep. Nat. Neurosci. *11*, 200–208.

28. Cai, D.J., Aharoni, D., Shuman, T., Shobe, J., Biane, J., Song, W., Wei, B., Veshkini, M., La-Vu, M., Lou, J., et al. (2016). A shared neural ensemble links distinct contextual memories encoded close in time. Nature *534*, 115–118.
29. de Bruin, J.P.C., Sànchez-Santed, F., Heinsbroek, R.P.W., Donker, A., and Postmes, P. (1994). A behavioural analysis of rats with damage to the medial prefrontal cortex using the Morris water maze: evidence for behavioural flexibility, but not for impaired spatial navigation. Brain Res. *652*, 323–333.
30. Tse, D., Takeuchi, T., Kakeyama, M., Kajii, Y., Okuno, H., Tohyama, C., Bito, H., and Morris, R.G.M. (2011). Schema-dependent gene activation and memory encoding in neocortex. Science *333*, 891–895.
31. Eichenbaum, H. (2017). Prefrontal-hippocampal interactions in episodic memory. Nat. Rev. Neurosci. *18*, 547–558.
32. Sekeres, M.J., Winocur, G., and Moscovitch, M. (2018). The hippocampus and related neocortical structures in memory transformation. Neurosci. Lett. *680*, 39–53.
33. Broadbent, N., Lumeij, L.B., Corcoles, M., Ayres, A.I., Bin Ibrahim, M.Z., Masatsugu, B., Moreno, A., Carames, J.M., Begg, E., Strickland, L., et al. (2020). A stable home-base promotes allocentric memory representations of episodic-like everyday spatial memory. Eur. J. Neurosci. *51*, 1539–1558.
34. Armbruster, B.N., Li, X., Pausch, M.H., Herlitze, S., and Roth, B.L. (2007). Evolving the lock to fit the key to create a family of G protein-coupled receptors potently activated by an inert ligand. Proc. Natl. Acad. Sci. USA *104*, 5163–5168.
35. Ghosh, K.K., Burns, L.D., Cocker, E.D., Nimmerjahn, A., Ziv, Y., Gamal, A.E., and Schnitzer, M.J. (2011). Miniaturized integration of a fluorescence microscope. Nat. Methods *8*, 871–878.
36. Chen, T.W., Wardill, T.J., Sun, Y., Pulver, S.R., Renninger, S.L., Baohan, A., Schreiter, E.R., Kerr, R.A., Orger, M.B., Jayaraman, V., et al. (2013). Ultrasensitive fluorescent proteins for imaging neuronal activity. Nature *499*, 295–300.
37. Zhou, P., Resendez, S.L., Rodriguez-Romaguera, J., Jimenez, J.C., Neufeld, S.Q., Giovannucci, A., Friedrich, J., Pnevmatikakis, E.A., Stuber, G.D., Hen, R., et al. (2018). Efficient and accurate extraction of *in vivo* calcium signals from microendoscopic video data. eLife *7*, e28728.
38. Runyan, C.A., Piasini, E., Panzeri, S., and Harvey, C.D. (2017). Distinct timescales of population coding across cortex. Nature *548*, 92–96.
39. Tintorelli, R., Budriesi, P., Villar, M.E., Marchal, P., da Cunha, P.L., Correa, J., Giurfa, M., and Viola, H. (2020). Spatial-memory formation after spaced learning involves ERKs1/2 activation through a behavioral-tagging process. Sci. Rep. *10*, 98.
40. Takeuchi, T., Duszkiewicz, A.J., Sonneborn, A., Spooner, P.A., Yamasaki, M., Watanabe, M., Smith, C.C., Fernández, G., Deisseroth, K., Greene, R.W., and Morris, R.G. (2016). Locus coeruleus and dopaminergic consolidation of everyday memory. Nature *537*, 357–362.
41. Pinto, L., and Dan, Y. (2015). Cell-type-specific activity in prefrontal cortex during goal-directed behavior. Neuron *87*, 437–450.
42. Euston, D.R., Gruber, A.J., and McNaughton, B.L. (2012). The role of medial prefrontal cortex in memory and decision making. Neuron *76*, 1057–1070.
43. Maviel, T., Durkin, T.P., Menzaghi, F., and Bontempi, B. (2004). Sites of neocortical reorganization critical for remote spatial memory. Science *305*, 96–99.
44. Scoville, W.B., and Milner, B. (1957). Loss of recent memory after bilateral hippocampal lesions. J. Neurol. Neurosurg. Psychiatry *20*, 11–21.
45. Maddock, R.J. (1999). The retrosplenial cortex and emotion: new insights from functional neuroimaging of the human brain. Trends Neurosci. *22*, 310–316.
46. Place, R., Farovik, A., Brockmann, M., and Eichenbaum, H. (2016). Bidirectional prefrontal-hippocampal interactions support context-guided memory. Nat. Neurosci. *19*, 992–994.
47. Czajkowski, R., Jayaprakash, B., Wiltgen, B., Rogerson, T., Guzman-Karlsson, M.C., Barth, A.L., Trachtenberg, J.T., and Silva, A.J. (2014). Encoding and storage of spatial information in the retrosplenial cortex. Proc. Natl. Acad. Sci. USA *111*, 8661–8666.
48. Milczarek, M.M., Vann, S.D., and Sengpiel, F. (2018). Spatial memory engram in the mouse retrosplenial cortex. Curr. Biol. *28*, 1975–1980.e6.
49. Bullitt, E. (1990). Expression of c-fos-like protein as a marker for neuronal activity following noxious stimulation in the rat. J. Comp. Neurol. *296*, 517–530.
50. Hintzman, D.L., Summers, J.J., and Block, R.A. (1975). Spacing judgments as an index of study-phase retrieval. J. Exp. Psychol. Hum. Learn. Mem. *1*, 31–40.
51. Redondo, R.L., and Morris, R.G.M. (2011). Making memories last: the synaptic tagging and capture hypothesis. Nat. Rev. Neurosci. *12*, 17–30.
52. Zong, W., Wu, R., Li, M., Hu, Y., Li, Y., Li, J., Rong, H., Wu, H., Xu, Y., Lu, Y., et al. (2017). Fast high-resolution miniature two-photon microscopy for brain imaging in freely behaving mice. Nat. Methods *14*, 713–719.
53. Schindelin, J., Arganda-Carreras, I., Frise, E., Kaynig, V., Longair, M., Pietzsch, T., Preibisch, S., Rueden, C., Saalfeld, S., Schmid, B., et al. (2012). Fiji: an open-source platform for biological-image analysis. Nat. Methods *9*, 676–682.
54. Pnevmatikakis, E.A., and Giovannucci, A. (2017). NoRMCorre: an online algorithm for piecewise rigid motion correction of calcium imaging data. J. Neurosci. Methods *291*, 83–94.
55. Glas, A., Hübener, M., Bonhoeffer, T., and Goltstein, P.M. (2019). Benchmarking miniaturized microscopy against two-photon calcium imaging using single-cell orientation tuning in mouse visual cortex. PLoS One *14*, e0214954.
56. Holtmaat, A., Bonhoeffer, T., Chow, D.K., Chuckowree, J., De Paola, V., Hofer, S.B., Hübener, M., Keck, T., Knott, G., Lee, W.C.A., et al. (2009). Long-term, high-resolution imaging in the mouse neocortex through a chronic cranial window. Nat. Protoc. *4*, 1128–1144.
57. Low, R.J., Gu, Y., and Tank, D.W. (2014). Cellular resolution optical access to brain regions in fissures: imaging medial prefrontal cortex and grid cells in entorhinal cortex. Proc. Natl. Acad. Sci. USA *111*, 18739–18744.
58. Weiler, S., Bauer, J., Hübener, M., Bonhoeffer, T., Rose, T., and Scheuss, V. (2018). High-yield *in vitro* recordings from neurons functionally characterized *in vivo*. Nat. Protoc. *13*, 1275–1293.
59. Franklin, K.B.J., and Paxinos, G. (2007). The Mouse Brain in Stereotaxic Coordinates (Academic Press Hardcover).

STAR★METHODS

KEY RESOURCES TABLE

REAGENT or RESOURCE	SOURCE	IDENTIFIER
Antibodies		
Rabbit anti-c-Fos	Synaptic Systems	Cat# 226 003; RRID: AB_2231974
Rabbit anti-Iba1	Wako	Cat# 019-19741; RRID: AB_839504
Chicken anti-GFAP	Abcam	Cat# ab4674; RRID: AB_304558
Bacterial and virus strains		
AAV2/1 CaMKII0.4-Cre	James M. Wilson, University of Pennsylvania	Addgene Cat# 105558-AAV1; RRID: Addgene_105558
AAV2/1 hSyn-flex-GCaMP6m	Douglas Kim & GENIE Project, Janelia Research Campus	Addgene Cat# 100838-AAV1; RRID: Addgene_100838
AAV2/9 hSyn-DIO-mCherry	Bryan Roth, University of North Carolina at Chapel Hill	Addgene Cat# 50459-AAV9; RRID: Addgene_50459
AAV2/9 hSyn-DIO-hM4D(Gi)-mCherry	Bryan Roth, University of North Carolina at Chapel Hill	Addgene Cat# 44362-AAV9; RRID: Addgene_44362
Chemicals, peptides, and recombinant proteins		
Fentanyl	HEXAL AG	N/A
Midazolam	Ratiopharm	N/A
Medetomidine	Vetoquinol GmbH	N/A
Lidocaine	AstraZeneca GmbH	N/A
Naloxone	Ratiopharm	N/A
Flumazenil	HEXAL AG	N/A
Atipamezole	Prodivet pharmaceuticals	N/A
Carprofen	Zoetis	N/A
Dexamethasone	Sigma	N/A
Clozapine-*N*-oxide	HelloBio	HB6149
Click-iT Plus TUNEL Assay	Thermo Fisher Scientific	C10617
Mounting medium with DAPI	Vector Laboratories	Cat# H-1200; RRID: AB_2336790
Experimental models: Organisms/strains		
Mice: C57BL/6NRj	Own breeding (origin: Jackson Laboratory)	Strain # 0664
Software and algorithms		
MATLAB R2016b	Mathworks	https://www.mathworks.com
LabVIEW 16.0	National Instruments	https://www.ni.com/en-us/shop/labview.html
Doric Neuroscience Studio 5.2.2.3	Doric Lenses	http://doriclenses.com/life-sciences/software/955-doric-neuroscience-studio.html
Python 3.5	Python Software Foundation	https://www.python.org
Behavioral tracker (version 1.0.0)	This paper; GitHub	https://github.com/pgoltstein/BehaviorTracker-8-arm-maze (https://doi.org/10.5281/zenodo.4984969)
Fiji (ImageJ) 1.52	[53]	https://imagej.net/Fiji
NoRMCorre	[54]	https://github.com/flatironinstitute/NoRMCorre
CNMF-E	[37]	https://github.com/zhoupc/CNMF_E
Custom analysis code (version 1.0.0)	This paper; GitHub	https://github.com/pgoltstein/everydaymemory-spacingeffect-mpfc (https://doi.org/10.5281/zenodo.4984961)

(*Continued on next page*)

Continued

REAGENT or RESOURCE	SOURCE	IDENTIFIER
Other		
Chocolate-flavored food pellets 97 mg	Bio-Serv	1818184
Prestige Muschelsand Kristal	Versele Laga	N/A
Miniaturized epifluorescence microscope	Doric Lenses	BFMS-S_UFGJ _1000_900_458
Microprism	IMM photonics	MPCH-1.5
Circular glass coverslip	Glaswarenfabrik Karl Hecht GmbH	4100110

RESOURCE AVAILABILITY

Lead contact

Further information and requests for resources and reagents should be directed to and will be fulfilled by the lead contact, Pieter M. Goltstein (goltstein@neuro.mpg.de).

Materials availability

This study did not generate new unique reagents or mouse lines.

Data and code availability

Main datasets generated during this study are available at https://gin.g-node.org/pgoltstein/everydaymemory-spacingeffect-mpfc/. Imaging data are available in the form of data processed using the CNMF-E algorithm (including the analysis options and settings). Main code supporting this study is available at https://github.com/pgoltstein/everydaymemory-spacingeffect-mpfc (https://doi.org/10.5281/zenodo.4984961). Additional requests for data and code should be directed to the lead contact, Pieter Goltstein (goltstein@neuro.mpg.de).

EXPERIMENTAL MODEL AND SUBJECT DETAILS

Female adult C57BL/6NRj mice were used (~postnatal day 90 at experimental onset). Female mice were used to minimize the possibility of intragroup aggression, ensuring that mice could be communally housed throughout the experiment, thus promoting animal wellbeing. Mice were communally housed in standard, individually ventilated cages (2–3 mice per cage), enriched with a running wheel, tunnel and shelter. Mice were kept on an inverted 12-h light, 12-h dark cycle with lights on at 10 or 11 PM (winter and summer time, respectively) with constant ambient temperature (~22°C) and humidity (~55%). Water was always available *ad libitum*. Prior to behavioral experiments, standard chow was available *ad libitum*. From the start of behavioral experiments, mice were food-restricted to 85% of their free-feeding weight. Littermates were randomly assigned to experimental groups. All procedures were performed in accordance with the institutional guidelines of the Max Planck Society and the regulations of the local government ethical committee (Beratende Ethikkommission nach §15 Tierschutzgesetz, Regierung von Oberbayern).

METHOD DETAILS

Surgical procedures

Mice were anesthetized with a mixture of fentanyl, midazolam and medetomidine in saline (FMM, 0.05 mg kg^{-1}, 5 mg kg^{-1}, and 0.5 mg kg^{-1} respectively, injected intraperitoneally). Lidocaine (10% w w^{-1}) was applied onto the scalp for topical anesthesia and carprofen (5 mg kg^{-1}, injected subcutaneously [s.c.]) was administered for analgesia. A head plate implantation was carried out as previously described.[55] For imaging experiments, a 3 mm circular craniotomy was created (centered at anteroposterior [AP] 2.0 mm, mediolateral [ML] 0.75 mm relative to bregma)[56] and a viral vector mixture of AAV2/1:CaMKII0.4-Cre ($4.6 \cdot 10^9$ genome copies [GC] ml^{-1}) and AAV2/1:hSyn-flex-GCaMP6m ($3.15 \cdot 10^{12}$ GC ml^{-1}) was unilaterally injected into the dmPFC at three injection sites along the anteroposterior axis (AP 1.6 mm, 2.0 mm, and 2.4 mm, ML 0.3 mm, dorsoventral [DV] −1.6 mm, 150 nL injection $^{-1}$, injection rate 25 nL min^{-1}). This sparse labeling approach facilitated detection of individual neuronal sources and restricted GCaMP6m expression to excitatory neurons. The left (n = 9 mice) or right (n = 10 mice) dmPFC was selected based on the superficial blood vessel pattern.

A microprism implant (comprised of an aluminum-coated, right-angle microprism [1.5 mm side length] glued to a circular glass window [3.0 mm diameter]) was implanted by removing the dura over one hemisphere and lowering the microprism into the sagittal fissure, facing the other hemisphere.[57] For chemogenetic inactivation experiments, a viral vector mixture of AAV2/1:CaMKII0.4-Cre ($2.1 \cdot 10^{11}$ GC ml^{-1}), and either AAV2/9:hSyn-DIO-mCherry ($2.1 \cdot 10^{12}$ GC ml^{-1}) or AAV2/9:hSyn-DIO-hM4D(Gi)-mCherry ($2.3 \cdot 10^{12}$ GC ml^{-1}) was bilaterally injected at two locations into the dmPFC (+2.5 mm AP, ± 0.3 mm ML, −1.0 mm DV, and +1.5 mm AP, ± 0.3 mm ML, −2.0 mm DV, relative to bregma; 150 nL injection^{-1}; injection rate 25 nL min^{-1}). Each viral vector injection was

flanked by a 5 min pre- and post-injection period. After surgery, anesthetic agents were antagonized with a mixture of naloxone, flumazenil and atipamezole in saline (NFA, 1.2 mg kg^{-1}, 0.5 mg kg^{-1}, and 2.5 mg kg^{-1} respectively, injected s.c.). Mice received carprofen (5 mg kg^{-1}, injected s.c.) and dexamethasone (2 mg kg^{-1}, injected s.c.) for two subsequent days. For imaging experiments, a second procedure was carried out two weeks after microprism placement in which a miniaturized microscope lens and adjustment ring were lowered and subsequently glued and cemented over the microprism implant (field of view center approximately at AP 2.2 mm [±300 μm], DV −0.8 mm [±200 μm]).

Behavioral procedures

Mouse handling, habituation, training, and testing was performed similarly as previously described,[7] with the main exception that training was conducted in a custom-made radial arm maze (Figure 1A). The maze was surrounded by multiple distal 3D cues and contained two proximal landmarks (Figure 1A). A remotely operated black Plexiglas start box was mounted at the end of one of the arms. The maze contained cutouts that contained either a sandwell (4 cm inner diameter, 4 cm depth, filled with sand and 5% w w^{-1} Garam Masala powder) or were covered by a white Plexiglas lid. The sandwells could not be seen from a distance from the mouse's perspective. The sandwells were subdivided in a center and surround compartment using semi-circular, perforated 3D-printed removable mesh cups. The surround compartment contained 20 chocolate-flavored pellets (97 mg, chocolate flavor) that served as masking odors and that were inaccessible to the mouse. During behavioral training, the rewarded sandwell contained one accessible chocolate-flavored pellet placed in the center compartment, 2 cm below the sand surface. In-between trials, all sandwells were refilled, any sand on the maze was brushed and vacuumed away, and all arms were carefully wiped with 40% ethanol. At the end of each day, the maze was thoroughly cleaned using 80% ethanol. Behavioral training was recorded with an overhead video camera and the frame-by-frame position of the mouse was automatically annotated using custom-written Python and MATLAB routines.

Behavioral experiments were conducted approximately between 12:00 and 19:00 o'clock. During the first 7 days of the experiment, the mice were habituated to the maze, habituated to carrying the miniaturized microscope, and trained to dig for a chocolate pellet in the sandwells. During the main experimental phase, each session typically consisted of three encoding trials (ETs) and three retrieval trials (RTs; Figure 1B; Video S1). The ETs had an encoding intertrial interval (ET_i) of either 30 s (“massed”), 10 min, 30 min, or 60 min (all “spaced”) and the retrieval delay (RT_d) between the final ET and first RT was 2.5 h or 24 h (Figure 1B). All eight combinations of ET_i and RT_d formed one session block and blocks were repeated either three (n = 10 mice) or five (n = 10 mice) times. The ET_i, RT_d, start box location, and the order in which the mice were tested were randomized across sessions. For a given mouse, the location of, and the egocentric path to, the rewarded sandwell was randomized across sessions.

At the start of an encoding trial, the mouse was placed into the start box for 60 s. Subsequently, the experimenter would remotely open the start box and the mouse could explore the maze containing the rewarded and non-rewarded sandwell. Once a mouse found the buried pellet, the mouse was gently nudged and went back to the start box where it consumed the reward. In sessions with an ET_i of 30 s, the door of the start box was opened after 30 s and two more encoding trials were conducted. At the end of the final ET_i, the mouse was kept in the start box for 60 s and subsequently placed back in its home cage. In sessions with an ET_i longer than 30 s, mice were placed back in the home cage after 60 s and remained there during the ET_i, after which two more encoding trials were conducted. Retrieval trials were conducted either 2.5 or 24 h after completion of the third encoding trial. In retrieval trials, the maze contained six sandwells: the rewarded sandwell, the non-rewarded sandwell, and four unfamiliar non-rewarded sandwells (“non-cued sandwells”). Training was carried out the same way as in encoding trials, except that the interval between subsequent retrieval trials was kept constant at 30 s.

As a second behavioral measure, evaluating memory acuity and strength, the first retrieval trial was occasionally replaced by a probe trial (Videos S2 and S3). A probe trial was conducted as a regular retrieval trial with the notable exception that the rewarded sandwell did not contain a reward for the first 60 s. After 60 s, the experimenter entered the maze room and placed one chocolate pellet in the sandwell. Probe trial sessions were interleaved with generally five but minimally two non-probe trial sessions.

After conclusion of the main behavioral training phase, several control experiments were conducted to evaluate whether mice could recall the rewarded location after a single encoding trial (Figures S1A–S1C), whether mice used an egocentric (Figures S2A and S2B) or allocentric (Figures S2C and S2D) navigation strategy, and to confirm the absence of primacy or recency effects (Figures S1D–S1F).

Immediate early gene expression

Mice were pseudo-randomly assigned to one of six groups, ensuring that cohoused mice were equally distributed across conditions. These groups underwent behavioral training using an ET_i of 30 s, 10 min, 30 min, or 60 min (Figure 2A), were placed in the maze for 1 min without training (“handled control”) or were merely handled (“home cage control”). Mice were kept in their home cage with litter mates and dim illumination after each encoding trial. Mice were perfused 90 min after handling (handled and home cage controls), after the start of ET2 (ET_i 30 s, 10 min, and 30 min), or 90 min after the middle of the interval between ET2 and ET3 (ET_i 60 min). As such, the time from ET3 to perfusion was 89 min, 80 min, 60 min, and 60 min for the groups undergoing behavioral training using ET_is of 30 s, 10 min, 30 min, and 60 min, respectively.

Chemogenetic inactivation

For *ex vivo* slice electrophysiology, reagent and brain tissue preparation were carried out as previously described.[58] Intracellular patch-clamp recordings were made on visually identified neurons expressing mCherry. We performed intracellular patch-clamp recordings using electrodes (3–5 MΩ) filled with K-gluconate-based internal solution[58] under continuous perfusion of carbogenated recording aCSF[58] (1 mL min^{-1}). Electrical signals were acquired using an amplifier, post-amplified, low-pass filtered (3 kHz cut-off), noise-filtered, digitized at 10 kHz, and recorded. To determine the effect of CNO on intrinsic excitability and current-evoked excitability of dmPFC excitatory neurons, two current injection protocols were executed (protocol 1: step: −100 pA prepulse injection for 100 ms, 500-ms delay, current injection ranging from −450 pA to 450 pA at steps of 50 pA for 750 ms; each step separated by 10 s; protocol 2: step: −100 pA prepulse injection for 100 ms, 500-ms delay, current injection ranging from 0 pA to 150 pA at steps of 10 pA for 750 ms; each step separated by 10 s). To assess the influence of CNO on the resting membrane potential, it was measured at 1 Hz intervals starting 5 min prior to influx of 50 μM CNO in recording aCSF until 10 min post-influx. Subsequently, both aforementioned step protocols were performed again. Recordings were carried out up to 12 h post-preparation. Only neurons whose series resistance did not change more than 20% during the recording were included in analysis.

In vivo chemogenetic inactivation experiments followed a full factorial 2^4 design, with the four factors protein expression (mCherry or hM4D(Gi)-mCherry conjugate), injection substance (saline [vehicle] or CNO in saline), injection time point (before an encoding trial or before a retrieval trial), and the session's ET_i (0.5 min or 60 min). For chemogenetic inactivation, mice were injected intraperitoneally with either vehicle or CNO (5 mg kg^{-1}) 45 min before behavioral testing (Figure 3A). Sessions with injections were conducted between 38 and 71 days after viral vector injection and were interleaved with at least two sessions without injections.

Histology and immunohistochemistry

Mice were deeply anesthetized with FMM and transcardially perfused with saline containing lidocaine and heparin (5 mg ml^{-1} and 2.8 mg ml^{-1}, respectively), followed by 4% PFA in PBS. Upon 72 h post-fixation in 4% PFA in PBS and cryoprotection in 30% sucrose for 72 h, brains were sectioned on a microtome (40 μm, coronal). For experiments quantifying immediate early gene expression, every 5^{th} section containing dmPFC was stained for c-Fos (rabbit anti-c-Fos [1:1000], followed by goat anti-rabbit Cy3 [1:200]) and mounted with mounting medium containing DAPI. For experiments quantifying injury caused by microprism implantation, every 5^{th} section containing dmPFC was stained for Iba1 (rabbit anti-Iba1 [1:1000], followed by goat anti-rabbit Cy3 [1:200]), or GFAP (chicken anti-GFAP [1:600], followed by goat anti-chicken Alexa 647 [1:200]), or Red TUNEL. Appropriate positive and negative controls were carried out for all stains.

For each slice containing the dmPFC (2.4 to 1.6 mm AP relative to bregma, 4 per mouse), five serial optical sections (spaced at 1 μm) of were acquired using a laser-scanning confocal microscope (TCS SP8, 20 × NA 0.75 objective). Images had a resolution of 1024 × 1024 pixels (550 × 550 μm) and color channels were acquired sequentially using excitation lasers for DAPI (excitation at 405 nm, emission at 410–419 nm) and Cy3 (excitation at 561 nm, emission at 575–714 nm).

Miniaturized microscopy

Sessions with simultaneous imaging were conducted between 20 and 98 days after viral vector injection. Images were acquired with a commercially available miniaturized microscope (Basic Fluorescence Microscopy System - Surface, Doric Lenses, excitation at 458/35 nm, emission at 525/40 nm) at a frame rate of 10 Hz and a resolution of 630 × 630 pixels (field of view ~1 mm^2). Laser power under the objective lens (2 × magnification, 0.5 NA) was < 1 mW for all imaging experiments. The miniaturized microscope body firmly docked into an implanted metal imaging cannula, thereby allowing reliable repositioning of the microscope over the same imaging field of view (Figure S5A).

QUANTIFICATION AND STATISTICAL ANALYSIS

Behavioral analysis

For each ET and RT, the number of erroneous sandwell digs were manually counted. Of note, multiple dig periods at the same incorrect sandwell were scored as one error. For each trial, the performance index was calculated as ($[error_{max} - error_{observed}] / error_{max} \cdot 100\%$), with $error_{max}$ being 1 for ETs and 5 for RTs. Retention was quantified as the relative difference in the mean PI of RT1 and ET3 for each individual mouse, across sessions of the same encoding intertrial interval and retrieval delay. For each probe trial, the time in the rewarded and non-rewarded arm was automatically recorded and behavioral videos were annotated frame-by-frame for position, speed, and distance to the nearest sandwell. Frames with mouse positions less than 1 cm from a sandwell and movement < 0.4 cm s^{-1} were labeled as dig frames. Performance in probe trials was quantified as the relative time spent digging at the rewarded sandwell as compared to the total dig time at both the rewarded and non-rewarded sandwell, i.e., the occupancy difference score ($ODS = dig_{rewarded} / [dig_{rewarded} + dig_{non\text{-}rewarded}]$).

Immunohistochemical analysis

Post-processing was conducted using ImageJ.[53] Serial optical sections (550 × 550 μm) were collapsed into one image and subsequently processed using the function "Subtract background" (rolling ball radius 10, sliding paraboloid), "Enhance contrast" (normalize, 0.1% saturated pixels), and rescaling brightness to the range of 0% to 78% of maximum brightness. Subsequently, a

blinded experimenter manually counted the number of immuno-positive neurons for each photomicrograph. These counts were subsequently multiplied by 3.25 and averaged to yield one measurement (1 mm^{-2}) per mouse.

Validation of microprism placement

For imaging experiments, the location of the microprism implant and viral vector transduction into the dmPFC were verified in coronal slices using a fluorescence microscope and compared to a reference atlas.[59]

Image processing and source extraction

Timing of individual behavioral video and miniaturized microscopy frames was synchronized using data acquisition cards. Behavioral data were downsampled to fit the miniaturized microscope frame acquisition rate. Using the NoRMCorre package[54] (specifiers: "*gSigma_align*" 9, "*gSize_align*" 25), frames within a single recording were first registered to each other and subsequently spatially and temporally downsampled to 256 × 256 pixels and 10 Hz. Multiple recordings of a single session were aligned and concatenated into a single stack. Single neuron Ca^{2+} activity traces were extracted from the fluorescent imaging time series by applying constrained nonnegative matrix factorization for microendoscopic data (CNMF-E)[37] using customized batch scripts (key specifiers median [±range]: "*gSigma_cnmfe*" 2, "*gSize_cnmfe*" 12, "*min_corr_cnmfe*" 0.75 [±0.1], "*min_pnr_cnmfe*" 8 [±2], "*edge_margin_cnmfe*" 8 [±3], "*merge_thr*" [.075, 0.75, 0], "*deconv_method*" constrained_foopsi; see Data and code availability). Putative sources that had less than six transients during a session or whose transients, fitted with a single-term exponential, had an exponential decay factor below −0.07 were removed. On average, we included 210 ± 99 neurons (mean ± SD) per session. All subsequent analyses were conducted using the deconvolved spike rate generated by the CNMF-E algorithm.

Quantification of p_{active}

To quantify the activity of a neuron during a trial, we used a probabilistic measure (p_{active}; Figure S6B). Trials were subdivided into the baseline period, i.e., the 60 s pre-trial period in the start box, and the trial period, from the first entry into the maze until 2 s after the mouse had retrieved the reward. Only trials with a minimum duration of 10 s were included in these analyses. To calculate p_{active}, a continuous, 5 s subsection was randomly selected from the baseline and trial period, thereby controlling for trial duration. The instantaneous inferred spike rate during both the baseline and trial subsection was averaged across the subsection. The average baseline inferred spike rate was subtracted from the average trial inferred spike rate, yielding the observed "trial activity rate". Subsequently, the trial activity rate was calculated 1000× using permuted spike rate data, and the resulting permuted trial activity rates were stored in a 1000 × 1 vector. If the observed trial activity rate was larger than the 95^{th} percentile of this vector, the neuron was labeled "active" for this particular 5 s subsection. The procedure outlined above was repeated 100 times for different, pseudo-randomly selected (i.e., non-duplicate) sections of baseline and trial periods. p_{active} was defined as the fraction of these 100 subsamples in which the neuron was labeled "active", and as such should be interpreted as the probability that a neuron was significantly more active during the trial as compared to the baseline period. This procedure was repeated for all neurons and all trials, and the p_{active} values were concatenated into an N × 1 vector (N = neurons), which was termed the ensemble response vector. We calculated the Pearson correlation coefficient between the ensemble response vectors of the six trials in a session, which yielded the ensemble correlation matrix.

Generalized linear model (GLM)

A GLM was fitted to the spiking activity of single neurons to establish the predictive power of specific behavioral parameters (task predictors; *tp*s) for neuronal activity, similar to approaches taken in Runyan et al.[38] (Figure 6A). The model incorporated the continuous task predictors running speed and running acceleration, and the categorical task predictors reward onset, reward anticipation (i.e., final entry into the rewarded arm), dig onset, dig offset, entry into the central platform, and intra-arm reversals of heading direction. Continuous task predictors were binned into 500 ms bins. Categorical task predictors were represented as boxcar functions [range 0,1], convolved with five evenly spaced Gaussian basis functions centered on the predictor onset (1.4 s half-width at half-height, peaks were spaced 2.5 s apart). Next, all predictors were rescaled to the range [0,1] and regularized using the MATLAB function "*lasso*" (specifiers: "*NumLambda*" 10, "*CV*" 10). Only regressors with non-zero regression coefficients at the minimum-deviance point were retained in the final, regularized model. The obtained regression coefficients were multiplied with the task predictor values and summed across temporally offset predictors of the same underlying task predictor. The regularized and deconvolved design matrix and a subsample of the neuron's inferred binarized spiking activity (70% of session's frames, downsampled to 2 Hz) were supplied to the MATLAB function "*fitglm*" (specifiers: "*modelspec*" linear, "*Distribution*" binomial, and "*link*" logit). When a resulting regression coefficient was significant on the t test after Bonferroni correction, the neuron was labeled "modulated" by this task predictor. To quantify model fit, the GLM was fitted to a permuted spike trace using the previously defined task predictors. Model fit was quantified as the adjusted R^2 of the model fitted to the observed spiking trace. The model's decoding performance was quantified by correlating the observed spiking responses (remaining 30% of session's frames) with the responses predicted by the GLM using the MATLAB function "*predict*".

Statistical analysis

Sample sizes were not estimated in advance. Animals were randomly assigned to experimental groups. No blinding was performed during experiments or data analysis, unless stated otherwise. All data are presented as mean (±SEM) unless stated otherwise.

Normality of distributions was assessed using the Kolmogorov-Smirnov test and appropriate parametric or non-parametric tests were used. Parametric analyses included the Student's t test (test statistic *t*) and general linear models including one-way repeated-measures (OWRM) or two-way repeated-measures (TWRM) ANOVA (test statistic *F*) for data consisting of two groups or more than two groups, respectively. To analyze probe trial performance, a one-sample t test against chance level 0 was conducted. Pooled data of the chemogenetic inactivation experiment were averaged per mouse, across injection time points and encoding intertrial intervals. To test the *a priori* hypothesis of a general effect of dmPFC inactivation, the chemogenetically inactivated group was directly compared to each of the three control groups using independent samples and paired samples t tests. The full 2^4 factorial dataset of the chemogenetic inactivation experiment was analyzed using a four-way mixed design (FWMD) ANOVA. To analyze the fractions of responsive neurons as detected by the GLM approach, a four-way (FW) ANOVA with session duration as a covariate was conducted to evaluate main effects only. Non-parametric analyses for data consisting of two groups included the Kolmogorov-Smirnov test (test statistic D), the Mann-Whitney U test (test statistic U), Spearman correlation (test statistic r_s) and the Wilcoxon's (matched-pairs) signed-rank test (test statistic W). The Kruskal-Wallis test (test statistic H) or Friedman's ANOVA (test statistic χ^2) was used for non-parametric analyses of data consisting of more than two groups. For all statistical tests, alpha was set at 0.05 and tests were conducted two-tailed unless stated otherwise. In case of multiple comparisons, a Bonferroni alpha correction was applied.

ADDITIONAL RESOURCES

Extended methodological descriptions are available at https://gin.g-node.org/pgoltstein/everydaymemory-spacingeffect-mpfc/.